Angewandte Communications

Gas-Phase Reactions

International Edition: DOI: 10.1002/anie.201503763
German Edition: DOI: 10.1002/ange.201503763

Distinct Mechanistic Differences in the Hydrogen-Atom Transfer from Methane and Water by the Heteronuclear Oxide Cluster $[Ga_2MgO_4]^{\bullet+}$**

*Jilai Li, Xiao-Nan Wu, Shaodong Zhou, Shiya Tang, Maria Schlangen, and Helmut Schwarz**

Dedicated to Professor Veronica Bierbaum on the occasion of her 65th birthday

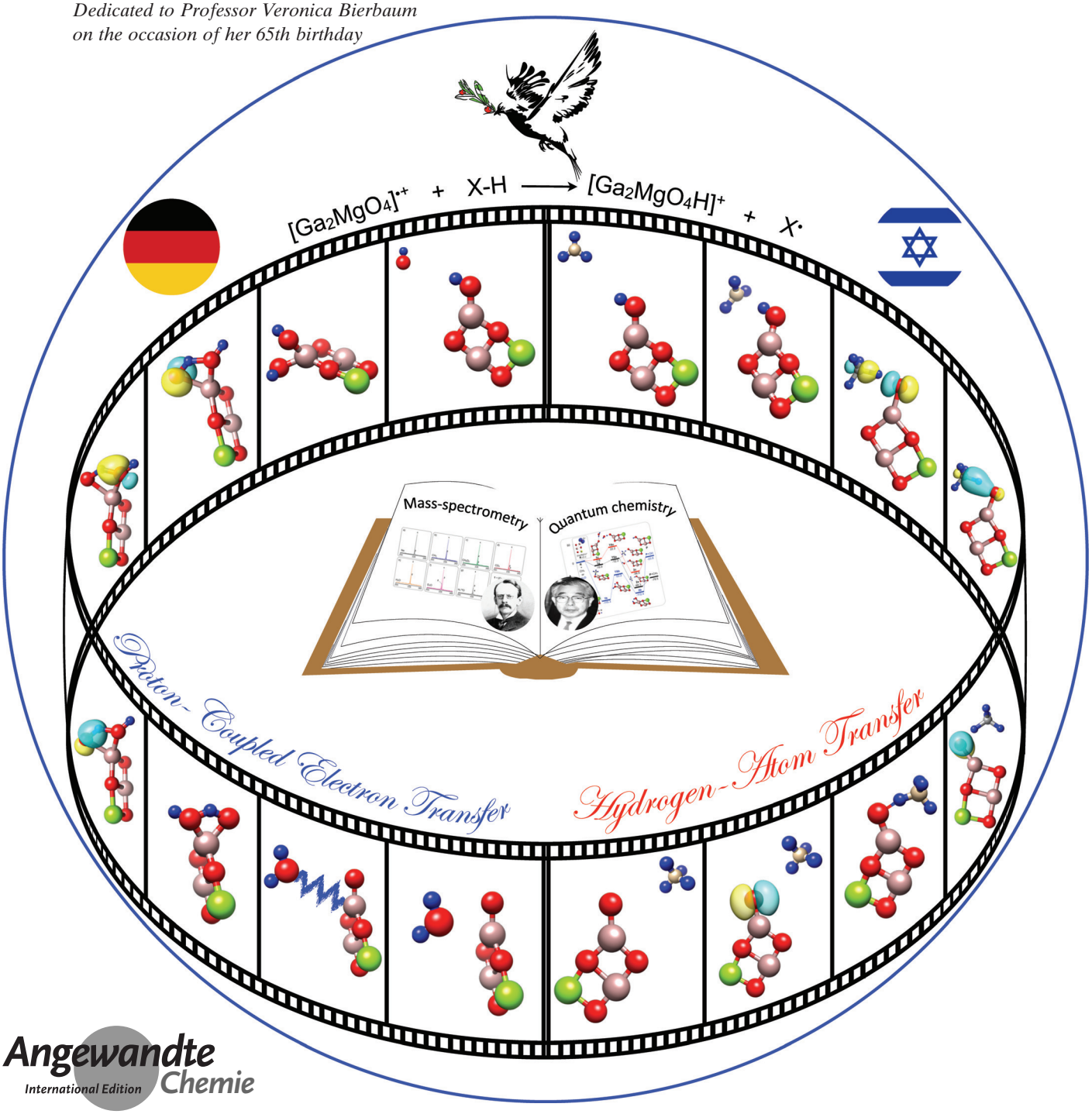

Abstract: *The thermal reactions of the heteronuclear oxide cluster $[Ga_2MgO_4]^{\bullet+}$ with methane and water have been studied using state-of-the-art gas-phase experiments in conjunction with quantum-chemical calculations. The significant reactivity differences, favoring activation of the strong O–H bond, can be ascribed to a proton-coupled electron transfer (PCET) mechanism operative in the activation of water. This study deepens our mechanistic understanding on how inert R–H bonds are cleaved by metal oxides.*

As the major component of natural gas, methane is abundant in nature and is regarded as an attractive building block for C_1 chemistry;[1] further, activation of this extremely inert hydrocarbon has attracted much attention not only because of the great economic interest, but also because of the inherent scientific challenges associated with this seemingly trivial transformation.[2] Water is the most ubiquitous compound on earth and its splitting constitutes a key step for capturing solar energy.[3] In addition, cleavage of the O–H bond in water by transition-metal compounds results in the generation of metal hydroxides or metal alkoxides.[3f,4] Metal alkoxides, and in particular, metal oxides have founded quite a few useful applications including their reactivity towards small, inert molecules, such as methane and water.[2c,e,5] While a mechanistic understanding of these reactions is of fundamental interest, many aspects remain to be elucidated in detail.[3e,5i,6]

Homolytic dissociation of the CH_3–H bond (439.3 kJ mol^{-1}) requires much less energy than that of the HO–H bond (497.1 kJ mol^{-1});[7] thus, whenever the activation of H_2O proceeds faster than that of CH_4, this may point to a fundamental mechanistic difference. Herein we describe the gas-phase reactions of the heteronuclear oxide cluster $[Ga_2MgO_4]^{\bullet+}$ with water and methane, examined by state-of-the-art mass-spectrometric experiments in conjunction with quantum-chemical calculations.[8] Implications derived from this combined experimental/computational investigation may provide mechanistic insights, which are a prerequisite for the rational design of low-molecular-weight catalysts.[2a,c,5a]

The Fourier transform ion-cyclotron resonance (FT-ICR) mass spectra in Figure 1 show the reactions of mass-selected, thermalized $[Ga_2MgO_4]^{\bullet+}$ ions (*m*/*z* 228; see the Supporting Information for details) with isotopomers of methane and water; mass spectra of the reaction with neon have also been recorded as reference spectra. As shown in Figure 1 a, the hydrogen-atom transfer (HAT) product ion $[Ga_2MgO_4H]^+$ is formed even when only neon is present in the ICR cell, revealing that $[Ga_2MgO_4]^{\bullet+}$ reacts with background impurities, such as water. Comparing the spectra in Figure 1 a–d, H-atom abstraction from methane [Eq. (1)] is clearly demonstrated. For example, the intensity of the product ion $[Ga_2MgO_4H]^+$ is much higher when methane is passed into the ICR cell (Figure 1 b). By correcting for the contribution of the reaction with the background, the rate constant $k([Ga_2MgO_4]^{\bullet+}/CH_4)$ is estimated to be 1.6×10^{-11} cm^3 molecule^{-1} s^{-1}, corresponding to a collision efficiency (ϕ) of 2%, relative to the collision rate;[9] the intramolecular kinetic isotope effect (KIE) derived from the $[Ga_2MgO_4]^{\bullet+}/CH_2D_2$ couple (Figure 1 c) and corrected for background contribution is 2.0. The O–H bond scission [Eq. (2a)) was confirmed in an isotopic labeling experiment with D_2O, in which the product ion $[Ga_2MgO_4D]^+$ is detected (Figure 1 f). When labeled $H_2{}^{18}O$ is introduced into the ICR cell, a signal with $\Delta m = +3$ relative to the precursor

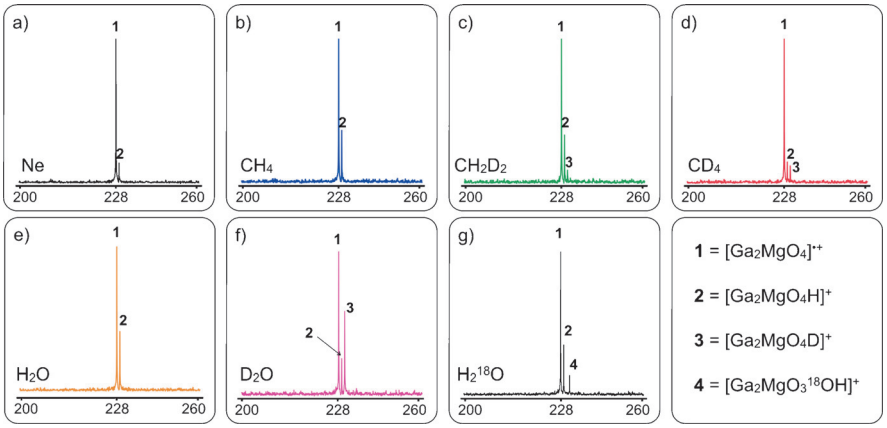

Figure 1. Mass spectra showing the reactivity of $[Ga_2MgO_4]^{\bullet+}$ with a) Ne, b) CH_4, c) CH_2D_2, and d) CD_4 at a pressure of 4.0×10^{-8} mbar and a reaction delay of 3 s, e) H_2O at a pressure of approximately 1.4×10^{-9} mbar after a reaction time of 3 s, f) D_2O at a pressure of approximately 2.5×10^{-9} mbar after a reaction time of 2 s, g) $H_2{}^{18}O$ at a pressure of approximately 1.0×10^{-9} mbar after a reaction time of 4 s. The occurrence of $[Ga_2MgO_4H]^+$ in (a) is caused by H-abstraction from background impurities, such as H_2O. See text for details. The unit for the *x* axes is always *m*/*z*.

$$[Ga_2MgO_4]^{\bullet+} + CH_4 \rightarrow [Ga_2MgO_4H]^+ + CH_3^{\bullet} \quad (1)$$

$$[Ga_2MgO_4]^{\bullet+} + H_2O \rightarrow [Ga_2MgO_4H]^+ + OH^{\bullet} \quad (2a)$$

[*] Dr. J. Li, Dr. X.-N. Wu, Dr. S. Zhou, Dr. S. Tang, Dr. M. Schlangen, Prof. Dr. H. Schwarz
Institut für Chemie
Technische Universität Berlin
Strasse des 17. Juni 135, 10623 Berlin (Germany)
E-mail: Helmut.Schwarz@tu-berlin.de
Dr. J. Li
Institute of Theoretical Chemistry, Jilin University
Changchun 130023 (People's Republic of China)

[**] This research was sponsored by the Deutsche Forschungsgemeinschaft (DFG), in particular the Cluster of Excellence "Unifying Concepts in Catalysis" (coordinated by the Technische Universität Berlin and funded by the DFG), and the Fonds der Chemischen Industrie. J.L. is grateful to "Unicat" for a postdoctoral fellowship. X.-N.W. appreciates support from the Alexander von Humboldt Foundation in the form of a postdoctoral research fellowship. We thank Dr. C. Geng and Dr. T. Weiske for helpful comments.

Supporting information for this article is available on the WWW under http://dx.doi.org/10.1002/anie.201503763.

$[Ga_2MgO_4]^{\bullet+}$ appears in addition to that for the product $[Ga_2MgO_4H]^+$ from the HAT from water (Figure 1g); this suggests the exchange of an oxygen atom between $H_2{}^{18}O$ and the oxide cluster concomitant with the transfer of a hydrogen atom [Eq. (2b)]. These ions are formed in primary reactions

$$[Ga_2MgO_4]^{\bullet+} + H_2{}^{18}O \rightarrow \begin{cases} [Ga_2MgO_3{}^{18}OH]^+ + OH^\bullet \\ [Ga_2MgO_4H]^+ + {}^{18}OH^\bullet \end{cases} \quad (2b)$$

as revealed by double-resonance experiments. In the double-resonance experiments, constant removal of the product ion $[Ga_2MgO_4H]^+$ from the reaction cell does not affect the formation of $[Ga_2MgO_3{}^{18}OH]^+$. In addition, the ratio of $[Ga_2MgO_3{}^{18}OH]^+$:$[Ga_2MgO_4H]^+$ is approximately 1:1, provided the intensity of $[Ga_2MgO_4H]^+$ as obtained from the reference spectra measured at the same pressure and with the same reaction delay is considered and corrected for. The rate constant $k([Ga_2MgO_4]^{\bullet+}/H_2O)$ is estimated to be 4.5×10^{-10} cm^3 molecule^{-1} s^{-1}, corresponding to a collision efficiency of $\phi = 25\,\%$.

Summarizing the experimental findings, it is clear that $[Ga_2MgO_4]^{\bullet+}$ activates both methane and water under thermal conditions, and the reactivity of the cluster toward H_2O is an order of magnitude higher than toward CH_4.

To obtain mechanistic insights into the $[Ga_2MgO_4]^{\bullet+}$-mediated C–H and O–H activations of methane and water, quantum-chemical calculations were carried out.[8c] The most favorable potential-energy surfaces of these reactions are shown in Figure 2, and relevant structural parameters are given in Table 1.

The most stable structure of $[Ga_2MgO_4]^{\bullet+}$ corresponds to a quasi-planar structure **R** (Figure 2 and Figure S1 in the Supporting Information) with the spin density localized on the terminal oxygen atom $O_t^{\bullet-}$. As shown in Figure 2, in the reaction of $[Ga_2MgO_4]^{\bullet+}$ with CH_4, an encounter complex **1a** is formed initially from the reactants (**R** and CH_4); this step is exothermic by −15 kJ mol^{-1}. Subsequently, one C–H bond is activated and the corresponding hydrogen atom is transferred to the $O_t^{\bullet-}$ unit of **R** via transition state **TSa** which is 12 kJ mol^{-1} lower in energy than the separated reactants. This process results in the formation of the association product **2a** (−98 kJ mol^{-1}), in which the methyl radical is loosely coordinated to the cluster by the H atom of the newly formed OH group. Finally, the hydroxide product ion

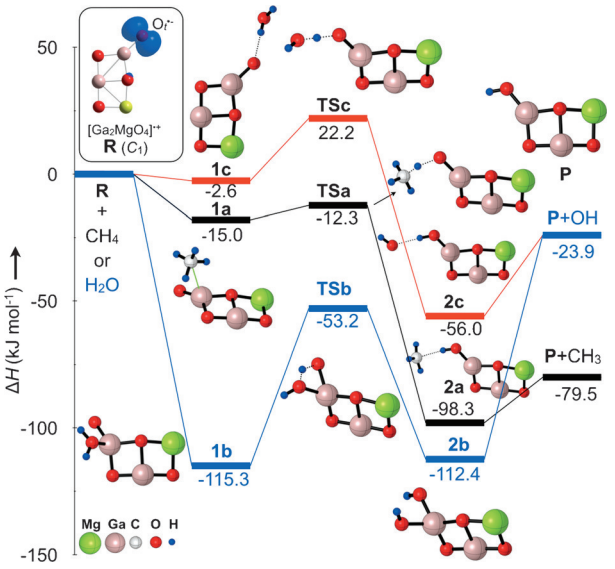

Figure 2. The potential energy surfaces (kJ mol^{-1}) and key ground-state structures involved in the reactions of $[Ga_2MgO_4]^{\bullet+}$ with CH_4 and H_2O calculated at the G4MP2-6X level of theory. The inset shows the ground-state structure of $[Ga_2MgO_4]^{\bullet+}$ (C_1 symmetry). The blue isosurface indicates the AIM-calculated spin-density distribution.

$[Ga_2MgO_4H]^+$ (**P**) is generated under release of a methyl radical. The rate-determining step corresponds to the formation of transition state **TSa** which is accessible under thermal conditions, in line with the experimental results.

Remarkably, a strikingly distinct reaction mechanism has been identified for the $[Ga_2MgO_4]^{\bullet+}/H_2O$ couple. As shown in Figure 2, a very stable encounter complex **1b** (−115 kJ mol^{-1}) is formed at the reaction entrance; interestingly, water does not directly approach the reactive oxygen atom but coordinates first to the metal center. Subsequently, the O–H activation proceeds via **TSb**, resulting in intermediate **2b**. Notably, **TSb** (−53 kJ mol^{-1}) is much lower in energy than the separated reactants, in contrast to **TSa** of the $[Ga_2MgO_4]^{\bullet+}/CH_4$ couple. There are two newly formed, structurally equivalent OH groups in **2b**, and release of OH yields the product ion **P** which is 24 kJ mol^{-1} lower in energy than the isolated reactants. The OH ligands in **2b** are indistinguishable, in line with the 1:1 ratio for the formation of $[Ga_2MgO_3{}^{18}OH]^+$

Table 1: Geometric parameters of stationary points in the reactions of $[Ga_2MgO_4]^{\bullet+}$ with methane and water calculated at the BMK/6-31+G(2df,p) level of theory. Bond lengths [Å] and bond angles [°]. For the reaction with water, O_t indicates the terminal oxygen atom of the cluster ion, O_w the oxygen atom of water.

	CH_4						H_2O				
Species	R_{Ga-O_t}	R_{O_t-H}	R_{C-H}	R_{Ga-C}	$\sphericalangle O_t$-H-C	Species	R_{Ga-O_t}	R_{O_t-H}	R_{O_w-H}	R_{Ga-O_w}	$\sphericalangle O_w$-H-O_t
R + CH_4	1.77	–	1.10	–	–	**R** + H_2O	1.77	–	0.96	–	–
1a	1.78	2.96	1.09	2.59	91.2	**1b**	1.80	2.84	0.97	1.99	80.7
						1c	1.77	2.10	0.96	4.53	180.0
TSa	1.76	1.49	1.16	3.33	165.7	**TSb**	1.95	1.24	1.24	1.86	134.2
						TSc	1.76	1.24	1.09	3.46	180.0
2a	1.73	0.97	2.13	4.06	172.2	**2b**	1.86	0.97	2.47	1.85	64.7
						2c	1.73	0.97	1.91	3.95	175.1
P + CH_3	1.74	0.96	–	–	–	**P** + OH	1.74	0.96	–	–	–

and $[Ga_2MgO_4H]^+$ in the labeling experiment described above. The rate-determining step corresponds to the cleavage of a Ga–O(H) bond with the concomitant release of OH. An alternative mechanism, similar to the one identified for the activation of CH_4, was also explored for the reaction of $[Ga_2MgO_4]^{\bullet+}$ with water in which the HAT reaction takes place by a direct approach of the substrate to the reactive oxygen atom of the cluster (**R** + H_2O → **1c**, Figure 2); however, this pathway encounters a prohibitively high barrier **TSc**, being 22 kJ mol^{-1} in energy higher than separated reactants. Thus, this reaction channel is not an option for O–H activation through this cluster under thermal conditions.

Regarding the structural features of the stationary points, the pathways of $[Ga_2MgO_4]^{\bullet+}/CH_4$ via **TSa** and $[Ga_2MgO_4]^{\bullet+}/H_2O$ via **TSc** are quite similar. As shown in Table 1, in the reaction of $[Ga_2MgO_4]^{\bullet+}$ with CH_4, the Ga–$O_t^{\bullet-}$ bond at the reactive site of the cluster and the C–H bond of methane remain almost intact: the Ga–$O_t^{\bullet-}$ bond is shortened by a negligible 0.02 Å (from 1.78 Å to 1.76 Å) and the C–H bond lengthened by only 0.07 Å (from 1.09 Å to 1.16 Å), in going from **1a** to **TSa**. This indicates an early transition state and thus a rather small intrinsic barrier (3 kJ mol^{-1}). Similarly, the Ga–$O_t^{\bullet-}$ bond length decreases also by only 0.01 Å in the reaction of $[Ga_2MgO_4]^{\bullet+}$ with H_2O in going from **1c** to the transition state **TSc**, and the activated O–H bond of water is lengthened by 0.13 Å (from 0.96 Å to 1.09 Å; Table 1). The different barrier heights of 3 kJ mol^{-1} and 19 kJ mol^{-1} for C–H and O–H activation via **TSa** and **TSc**, respectively, can be explained by the different increments of stretching the C–H (5%) versus O–H (14%) bonds in **TSa** versus **TSc** and their different bond dissociation energies as noted above. This results in an apparent barrier for the O–H activation via **TSc** which cannot be surmounted under thermal conditions.

The different energy pattern of the C–H and O–H activations via **TSa** and **TSb** can also be explained based on an inspection of the structural features. In sharp contrast to the features noted above for the C–H activation for the $[Ga_2MgO_4]^{\bullet+}/CH_4$ couple, in the $[Ga_2MgO_4]^{\bullet+}/H_2O$ system the Ga–$O_t^{\bullet-}$ bond at the reactive site of the cluster as well as the O–H bond of water lengthen by 0.15 Å (from 1.80 Å to 1.95 Å; Table 1) and by 0.27 Å (from 0.97 Å to 1.24 Å), respectively, in going from **1b** to **TSb**. These dramatic bond elongations, especially for the stronger O–H bond of H_2O, account for the considerably higher intrinsic barrier for the O–H activation via **TSb**. Further, the relatively high energy difference between the two encounter complexes **1a** and **1b** with an energy preference of 100 kJ mol^{-1} in favor of **1b** can be attributed to the strong interaction between the Ga atom at the reactive site and the oxygen atom of H_2O: the calculated Wiberg bond index of the Ga–C bond in **1a** amounts to only 0.08, whereas a value of 0.24 is obtained for the Ga–O_w bond in **1b**. In contrast to the strong ion–dipole interaction between the Ga atom and O_w, only a rather weak dispersion interaction between the cluster and the incoming water exists in **1c**.

A frontier-molecular-orbital analysis on the electron-density development has been performed to provide further details and insight.[10] As shown in Figure 3, $[Ga_2MgO_4]^{\bullet+}$ reacts with CH_4 in a standard HAT mechanism.[11] Three

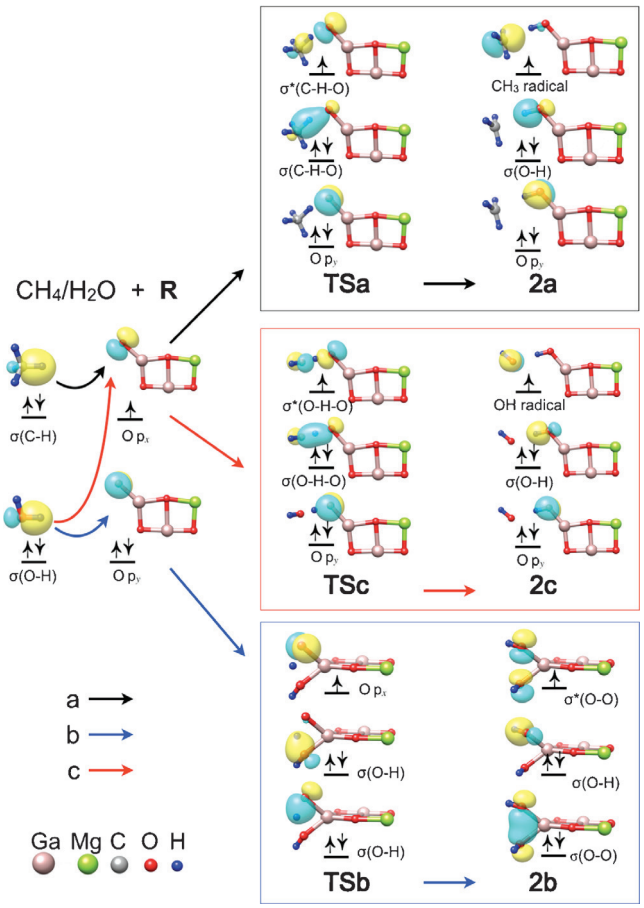

Figure 3. Schematic MO diagrams for homolytic HAT from methane (black), or water (red), and PCET from water (blue). For the sake of clarity, the structures of **TSb** and **2b** were rotated by 90° around the $Ga_{(Ot)}$–Mg axis.

electrons are delocalized over the C-H-O moiety in the transition state **TSa**; one of the electrons is contributed by the $O_t^{\bullet-}$ radical (O p_x in **R**) and two by the σ(C–H) bond of CH_4. **TSa** is characterized by a 3-electron/3-center bond with a doubly occupied bonding orbital along the C-H-O axis, σ(C-H-O), and a singly occupied antibonding orbital, σ*(C-H-O); the doubly occupied p_y orbital of $O_t^{\bullet-}$ is perpendicular to the C-H-O axis and acts as a spectator. Similarly, the reaction of $[Ga_2MgO_4]^{\bullet+}$ with H_2O via a collinear O-H-O arrangement, to proceed via **TSc**, also corresponds to a standard HAT mechanism. However, as mentioned above there is an alternative pathway for the activation of the O–H bond for the $[Ga_2MgO_4]^{\bullet+}/H_2O$ couple. Thus, to avoid the rather high promotion energy required to transfer an electron from the σ(O–H) bond orbital to O p_x, the electron pair located in O p_y abstracts a proton from the σ(O–H) bond of H_2O; thus, four electrons end up in two strong σ(O–H) bonds of transition state **TSb** in which, O p_x is perpendicular to the O-H-O axis and is singly occupied in both the reactant **R** as well as in **TSb**. In **2b**, the unpaired electron is equally delocalized in a σ*(O–O) orbital over the H-abstracting oxygen atom and the oxygen atom of the water moiety. Thus, this reaction path has features of a proton-coupled electron transfer (PCET) with the net effect of a HAT.[11b,12]

In summary, in this study we demonstrated that the activation of methane and water by the heteronuclear oxide cluster $[Ga_2MgO_4]^{\bullet+}$ proceeds by distinctly different mechanisms. The higher reactivity of $[Ga_2MgO_4]^{\bullet+}$ towards the stronger O–H bond of water is due to a proton-coupled electron transfer mechanism; this is beneficial to lower the rate-determining transition state by avoiding the population of a relatively high-lying, singly occupied O p_x orbital. In contrast, activation of methane does not have this option but rather involves the classical homolytic hydrogen-atom transfer for which the high spin density at the terminal $O_t^{\bullet-}$ unit of the cluster ion matters.[11]

Keywords: bond activation · computational chemistry · gas-phase reactions · mass spectrometry · radicals

How to cite: *Angew. Chem. Int. Ed.* **2015**, *54*, 12298–12302
Angew. Chem. **2015**, *127*, 12298–12477

[1] a) G. A. Olah, A. Goeppert, G. K. S. Prakash, *J. Org. Chem.* **2009**, *74*, 487–498; b) G. A. Olah, *Angew. Chem. Int. Ed.* **2005**, *44*, 2636–2639; *Angew. Chem.* **2005**, *117*, 2692–2696.

[2] a) H. Schwarz, *Angew. Chem. Int. Ed.* **2015**, DOI: 10.1002/anie.201500649; *Angew. Chem.* **2015**, DOI: 10.1002/ange.201500649; b) R. Horn, R. Schlögl, *Catal. Lett.* **2015**, *145*, 23–39; c) H. Schwarz, *Isr. J. Chem.* **2014**, *54*, 1413–1431; d) P. Schwach, M. G. Willinger, A. Trunschke, R. Schlögl, *Angew. Chem. Int. Ed.* **2013**, *52*, 11381–11384; *Angew. Chem.* **2013**, *125*, 11591–11594; e) H. Schwarz, *Angew. Chem. Int. Ed.* **2011**, *50*, 10096–10115; *Angew. Chem.* **2011**, *123*, 10276–10297; f) J. Roithová, D. Schröder, *Chem. Rev.* **2010**, *110*, 1170–1211; g) R. H. Crabtree, *Chem. Rev.* **1995**, *95*, 2599–2599; h) B. A. Arndtsen, R. G. Bergman, T. A. Mobley, T. H. Peterson, *Acc. Chem. Res.* **1995**, *28*, 154–162.

[3] a) M. D. Kärkäs, O. Verho, E. V. Johnston, B. Åkermark, *Chem. Rev.* **2014**, *114*, 11863–12001; b) D. Cappelletti, E. Ronca, L. Belpassi, F. Tarantelli, F. Pirani, *Acc. Chem. Res.* **2012**, *45*, 1571–1580; c) H. Dau, C. Limberg, T. Reier, M. Risch, S. Roggan, P. Strasser, *ChemCatChem* **2010**, *2*, 724–761; d) P. J. Roach, W. H. Woodward, A. W. Castleman, A. C. Reber, S. N. Khanna, *Science* **2009**, *323*, 492–495; e) M. Yagi, M. Kaneko, *Chem. Rev.* **2001**, *101*, 21–36; f) O. Blum, D. Stöckigt, D. Schröder, H. Schwarz, *Angew. Chem. Int. Ed. Engl.* **1992**, *31*, 603–604; *Angew. Chem.* **1992**, *104*, 637–639.

[4] M. Brönstrup, D. Schröder, H. Schwarz, *Chem. Eur. J.* **1999**, *5*, 1176–1185.

[5] a) J. Li, X.-N. Wu, M. Schlangen, S. Zhou, P. González-Navarrete, S. Tang, H. Schwarz, *Angew. Chem. Int. Ed.* **2015**, *54*, 5074–5078; *Angew. Chem.* **2015**, *127*, 5163–5167; b) L.-N. Wang, Z.-X. Zhou, X.-N. Li, T.-M. Ma, S.-G. He, *Chem. Eur. J.* **2015**, *21*, 6957–6961; c) X.-N. Wu, S.-Y. Tang, H.-T. Zhao, T. Weiske, M. Schlangen, H. Schwarz, *Chem. Eur. J.* **2014**, *20*, 6672–6677; d) J.-H. Meng, X.-J. Deng, Z.-Y. Li, S.-G. He, W.-J. Zheng, *Chem. Eur. J.* **2014**, *20*, 5580–5583; e) J.-B. Ma, Z.-C. Wang, M. Schlangen, S.-G. He, H. Schwarz, *Angew. Chem. Int. Ed.* **2013**, *52*, 1226–1230; *Angew. Chem.* **2013**, *125*, 1264–1268; f) N. Dietl, X. H. Zhang, C. van der Linde, M. K. Beyer, M. Schlangen, H. Schwarz, *Chem. Eur. J.* **2013**, *19*, 3017–3028; g) Z.-C. Wang, J.-W. Liu, M. Schlangen, T. Weiske, D. Schröder, J. Sauer, H. Schwarz, *Chem. Eur. J.* **2013**, *19*, 11496–11501; h) R. Kretschmer, M. Schlangen, H. Schwarz, *Angew. Chem. Int. Ed.* **2013**, *52*, 6097–6101; *Angew. Chem.* **2013**, *125*, 6213–6217; i) Z.-C. Wang, T. Weiske, R. Kretschmer, M. Schlangen, M. Kaupp, H. Schwarz, *J. Am. Chem. Soc.* **2011**, *133*, 16930–16937; j) N. P. R. Dietl, M. Schlangen, H. Schwarz, *Chem. Eur. J.* **2011**, *17*, 1783–1788; k) N. Dietl, R. F. Höckendorf, M. Schlangen, M. Lerch, M. K. Beyer, H. Schwarz, *Angew. Chem. Int. Ed.* **2011**, *50*, 1430–1434; *Angew. Chem.* **2011**, *123*, 1466–1470; l) N. Dietl, R. Paul, C. Linde, M. Schlangen, M. K. Beyer, H. Schwarz, *Angew. Chem. Int. Ed.* **2011**, *50*, 4966–4969; *Angew. Chem.* **2011**, *123*, 5068–5072; m) K. Chen, Z.-C. Wang, M. Schlangen, Y.-D. Wu, X. Zhang, H. Schwarz, *Chem. Eur. J.* **2011**, *17*, 9619–9625; n) U. Zavyalova, G. Weinberg, W. Frandsen, F. Girgsdies, T. Risse, K. P. Dinse, R. Schloegl, R. Horn, *ChemCatChem* **2011**, *3*, 1779–1788; o) U. Zavyalova, M. Geske, R. Horn, G. Weinberg, W. Frandsen, M. Schuster, R. Schlögl, *ChemCatChem* **2011**, *3*, 949–959; p) S. Feyel, D. Schröder, H. Schwarz, *Eur. J. Inorg. Chem.* **2008**, 4961–4967.

[6] a) J.-B. Ma, Y.-X. Zhao, S.-G. He, X.-L. Ding, *J. Phys. Chem. A* **2012**, *116*, 2049–2054; b) Z. C. Wang, N. Dietl, R. Kretschmer, J. B. Ma, T. Weiske, M. Schlangen, H. Schwarz, *Angew. Chem. Int. Ed.* **2012**, *51*, 3703–3707; *Angew. Chem.* **2012**, *124*, 3763–3767; c) J.-B. Ma, Z.-C. Wang, M. Schlangen, S.-G. He, H. Schwarz, *Angew. Chem. Int. Ed.* **2012**, *51*, 5991–5994; *Angew. Chem.* **2012**, *124*, 6093–6096; d) N. P. R. Dietl, M. Engeser, H. Schwarz, *Angew. Chem. Int. Ed.* **2009**, *48*, 4861–4863; *Angew. Chem.* **2009**, *121*, 4955–4957; e) S. Feyel, J. Döbler, R. F. Höckendorf, M. K. Beyer, J. Sauer, H. Schwarz, *Angew. Chem. Int. Ed.* **2008**, *47*, 1946–1950; *Angew. Chem.* **2008**, *120*, 1972–1976; f) S. Feyel, J. Döbler, D. Schröder, J. Sauer, H. Schwarz, *Angew. Chem. Int. Ed.* **2006**, *45*, 4681–4685; *Angew. Chem.* **2006**, *118*, 4797–4801; g) B. C. Garrett, D. A. Dixon, D. M. Camaioni, D. M. Chipman, M. A. Johnson, C. D. Jonah, G. A. Kimmel, J. H. Miller, T. N. Rescigno, P. J. Rossky, S. S. Xantheas, S. D. Colson, A. H. Laufer, D. Ray, P. F. Barbara, D. M. Bartels, K. H. Becker, K. H. Bowen, S. E. Bradforth, I. Carmichael, J. V. Coe, L. R. Corrales, J. P. Cowin, M. Dupuis, K. B. Eisenthal, J. A. Franz, M. S. Gutowski, K. D. Jordan, B. D. Kay, J. A. LaVerne, S. V. Lymar, T. E. Madey, C. W. McCurdy, D. Meisel, S. Mukamel, A. R. Nilsson, T. M. Orlando, N. G. Petrik, S. M. Pimblott, J. R. Rustad, G. K. Schenter, S. J. Singer, A. Tokmakoff, L.-S. Wang, T. S. Zwier, *Chem. Rev.* **2005**, *105*, 355–390; h) G. K. Koyanagi, D. K. Bohme, I. Kretzschmar, D. Schröder, H. Schwarz, *J. Phys. Chem. A* **2001**, *105*, 4259–4271.

[7] a) D. M. Golden, S. W. Benson, *Chem. Rev.* **1969**, *69*, 125–134; b) J. A. Kerr, *Chem. Rev.* **1966**, *66*, 465–500.

[8] a) J. L. Li, R. A. Mata, U. Ryde, *J. Chem. Theory Comput.* **2013**, *9*, 1799–1807; b) X. Zhang, H. Schwarz, *Theor. Chem. Acc.* **2011**, *129*, 389–399; c) B. Chan, J. Deng, L. Radom, *J. Chem. Theory Comput.* **2010**, *7*, 112–120; d) J. Li, C. Geng, X. Huang, C. Sun, *J. Chem. Theory Comput.* **2006**, *2*, 1551–1564.

[9] a) G. Kummerlöwe, M. K. Beyer, *Int. J. Mass Spectrom.* **2005**, *244*, 84–90; b) T. Su, M. T. Bowers, *J. Chem. Phys.* **1973**, *58*, 3027–3037; c) M. T. Bowers, J. B. Laudenslager, *J. Chem. Phys.* **1972**, *56*, 4711–4712.

[10] a) X. Sun, C. Geng, R. Huo, U. Ryde, Y. Bu, J. Li, *J. Phys. Chem. B* **2014**, *118*, 1493–1500; b) X. Sun, X. Sun, C. Geng, H. Zhao, J. Li, *J. Phys. Chem. A* **2014**, *118*, 7146–7158; c) J. L. Li, X. Zhang, X. R. Huang, *Phys. Chem. Chem. Phys.* **2012**, *14*, 246–256; d) X. L. Sun, X. R. Huang, J. L. Li, R. P. Huo, C. C. Sun, *J. Phys. Chem. A* **2012**, *116*, 1475–1485; e) C. Y. Geng, S. Ye, F. Neese, *Angew. Chem. Int. Ed.* **2010**, *49*, 5717–5720; *Angew. Chem.* **2010**, *122*, 5853–5856; f) K. Fukui, *Science* **1982**, *218*, 747–754.

[11] a) N. Dietl, M. Schlangen, H. Schwarz, *Angew. Chem. Int. Ed.* **2012**, *51*, 5544–5555; *Angew. Chem.* **2012**, *124*, 5638–5650; b) W. Lai, C. Li, H. Chen, S. Shaik, *Angew. Chem. Int. Ed.* **2012**, *51*, 5556–5578; *Angew. Chem.* **2012**, *124*, 5652–5676.

[12] a) J. M. Mayer, *Acc. Chem. Res.* **2011**, *44*, 36–46; b) C. T. Saouma, J. M. Mayer, *Chem. Sci.* **2014**, *5*, 21–31.

Received: April 24, 2015
Published online: July 1, 2015

